Scientific Research Publishing

Open Journal of Radiology, 2023, 13, 101-112
https://www.scirp.org/journal/ojrad
ISSN Online: 2164-3032
ISSN Print: 2164-3024

Image-Based Ultrasound Speed Estimation: Phantom and Human Liver Studies

Jianfeng Chen*, Junguo Bian, Zuhaib Khokhar, Mohamed Belal, Emad Allam

Department of Radiology and Medical Imaging, Stritch School of Medicine, Loyola University Medical Center, Chicago, Illinois, USA
Email: *jfchen@live.com

How to cite this paper: Chen, J.F., Bian, J.G., Khokhar, Z., Belal, M. and Allam, E. (2023) Image-Based Ultrasound Speed Estimation: Phantom and Human Liver Studies. *Open Journal of Radiology*, **13**, 101-112.
https://doi.org/10.4236/ojrad.2023.132011

Received: May 16, 2023
Accepted: June 27, 2023
Published: June 30, 2023

Abstract

Purpose: A novel image-based method for speed of sound (SoS) estimation is proposed and experimentally validated on a tissue-mimicking ultrasound phantom and normal human liver *in vivo* using linear and curved array transducers. **Methods:** When the beamforming SoS settings are adjusted to match the real tissue's SoS, the ultrasound image at regions of interest will be in focus and the image quality will be optimal. Based on this principle, both a tissue-mimicking ultrasound phantom and normal human liver *in vivo* were used in this study. Ultrasound image was acquired using different SoS settings in beamforming channels ranging from 1420 m/sec to 1600 m/sec. Two regions of interest (ROIs) were selected. One was in a fully developed speckle region, while the other contained specular reflectors. We evaluated the image quality of these two ROIs in images acquired at different SoS settings in beamforming channels by using the normalized autocorrelation function (ACF) of the image data. The values of the normalized ACF at a specific lag as a function of the SoS setting were computed. Subsequently, the soft tissue's SoS was determined from the SoS setting at the minimum value of the normalized ACF. **Results:** The value of the ACF as a function of the SoS setting can be computed for phantom and human liver images. SoS in soft tissue can be determined from the SoS setting at the minimum value of the normalized ACF. The estimation results show that the SoS of the tissue-mimicking phantom is 1460 m/sec, which is consistent with the phantom manufacturer's specification, and the SoS of the normal human liver is 1540 m/sec, which is within the range of the SoS in a healthy human liver *in vivo*. **Conclusion:** Soft tissue's SoS can be determined by analyzing the normalized ACF of ultrasound images. The method is based on searching for a minimum of the normalized ACF of ultrasound image data with a specific lag among different SoS settings in beamforming channels.

Keywords

Ultrasound Image, Normalized Autocorrelation Function (ACF), Speed of Sound (SoS)

1. Introduction

Clinical ultrasound imaging systems usually assume that the speed of sound (SoS) in soft-tissues is constant, mostly 1540 m/s, so that the sound waves in the soft-tissue can be focused by simply delaying and summing according to known geometric distances and the SoS in the tissue. Ideally, if the SoS set in beamforming channels matches the true SoS in the tissue, both the transmitted and received signals should be well aligned after applying the time delays. However, the difference between the SoS in the tissue and in the beamforming channels will cause ultrasound signal misalignment of the beamforming channels and thereby degrade both the spatial resolution and the sensitivity of ultrasound images. Moreover, if there is some in homogeneity of SoS in the soft-tissues, higher-order phase aberrations can further lead to signal misalignment after geometric delays are applied and lead to further degradation of the ultrasound image quality [1] [2] [3] [4].

A concept to estimate the SoS in soft tissue by using ultrasound was proposed by Chen *et al.* [5]. When soft tissue was scanned by an ultrasound imaging system, a series of ultrasound images were created by using different SoS settings in beamforming channels. Then, an image quality function that is indicative of image quality at a specific region of interest (ROI) was computed. That function could exhibit a minimum or maximum value when the SoS setting in beamforming channels equals a true SoS in the tissue. A method to select the SoS automatically in order to improve lateral resolution in the resulting image was developed by Napolitano *et al.* [4] [6] [7]. This is done by analyzing the spatial frequency data of images reconstructed with various sound speeds. The main limitation of the method is that the image must contain an isolated feature. This concept was then applied to photo acoustic tomography of soft tissues [8] in order to obtain an average SoS that can maximize the image sharpness. This method eliminates the need of a priori knowledge, such as the geometry of a calibration block or a reference image for comparison.

In this paper we propose a method based on the normalized autocorrelation function (ACF) of image data for averaged SoS estimation. The method works well under weaker constraints, *i.e.*, no assumption of isolated image features, whether for speckle, the appearance of texture due to ultrasound scattering from a set of diffuse small scattering structures within a specific tissue, or the specular reflector with structure scale larger than the ultrasound wavelength. This study is organized as follows: In Section 2, a method based on the normalized ACF of image data for averaged SoS is presented; in Section 3, the experiments set up for

both a tissue mimicking phantom and healthy liver images *in vivo* are described; in Section 4, the test results are discussed and summarized. Section 5 presents the final conclusions.

2. Method

In our study, an ultrasound tissue mimicking phantom (Multipurpose Phantom Model 539, ATS Laboratories Incorporated, Bridgeport, CT) and a normal human liver were used in this study. A GE LOGIQ E9 scanner with a ML6-15 linear array transducer at 10 MHz and C1-6 curved array transducer at 3.5 MHz were used. As shown in Figure 1, a series of ultrasound images were generated by using different SoS settings in beamforming channels. The SoS settings were ranged from 1420 m/sec to 1620 m/sec. In our phantom study, two ROIs were selected among those ultrasound images, as shown in Figure 2. One was located in a fully developed speckle area with an image size of 150 × 50 pixels, while other contained a specular reflector with the same size of 150 × 50 pixels using the ML6-15 linear array. In our human liver study, two ROIs with the same size

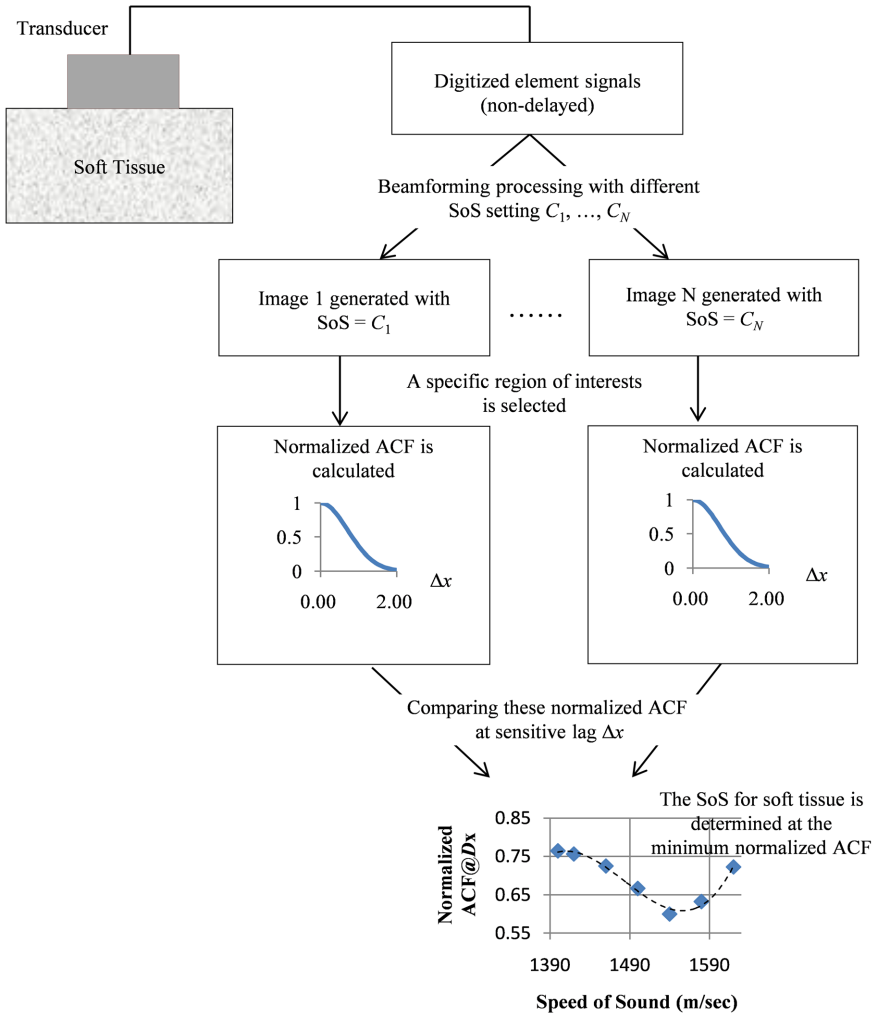

Figure 1. Block diagram of the image-based SoS estimation method.

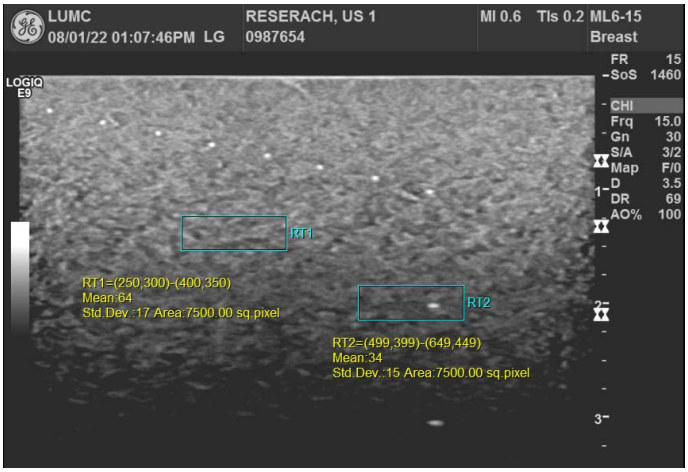

Figure 2. Two ROIs were selected on a typical ultrasound phantom image. One region contains fully developed speckle, while the other region contains a specular reflector.

of 200 × 50 pixels (ML6-15 linear transducer) and 100 × 100 pixels (C1-6 curved array transducer) were selected respectively, one was within a fully-developed speckle area, while the other contained some specular structures as shown in **Figure 3** and **Figure 4**. Image pixel size was 0.089 mm for the ML6-15 linear array and 0.25 mm for the C1-6 curved array transducer.

Subsequently, we can evaluate the image quality by using a normalized ACF of image data over these ROIs. Here the normalized ACF is defined by

$$\mathrm{ACF}(\Delta x)=\frac{\sum_{i=1}^{M}\sum_{j=1}^{N}\left[\left(I\left(x_i,y_j\right)-\langle I\rangle\right)*\left(I\left(x_i+\Delta x,y_j\right)-\langle I\rangle\right)\right]}{\sum_{i=1}^{M}\sum_{j=1}^{N}\left[I\left(x_i,y_j\right)-\langle I\rangle\right]^2}$$

where

$I\left(x_i,y_j\right)$ is the ultrasound image signal intensity at location $\left(x_i,y_j\right)$,

x is in the lateral direction and y is in the depth direction,

$M\times N$ is the total number of data pairs $I\left(x_i,y_j\right)$ and $I\left(x_i+\Delta x,y_j\right)$ in aROI,

Δx is the lag distance between two positions $\left(x_i,y_j\right)$ and $\left(x_i+\Delta x,y_j\right)$ in the lateral direction, which is perpendicular to the depth direction ofultrasound image, and

$\langle I\rangle$ is the mean of image intensity within ROI and is given by

$$\langle I\rangle=\frac{\sum_{i=1}^{M}\sum_{j=1}^{N}I\left(x_i,y_j\right)}{M\times N}.$$

The shape of a typical normalized ACF for ultrasound image data is approximately Gaussian, as shown in **Figure 5(a)**. The steepest slope of the normalized ACF, corresponding to a second derivative of zero, will be the most sensitive point where a change in lag will result in the largest change in ACF, as shown in **Figure 5(b)**. If the shape of the normalized ACF is given by $y=\mathrm{e}^{-a\Delta x^2}$, then based on $y''=0$, we have the most sensitive lag, Δx, which satisfies the following equation:

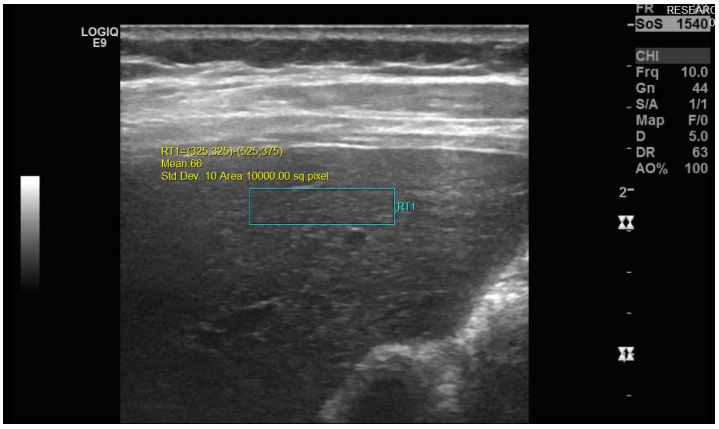

(a)

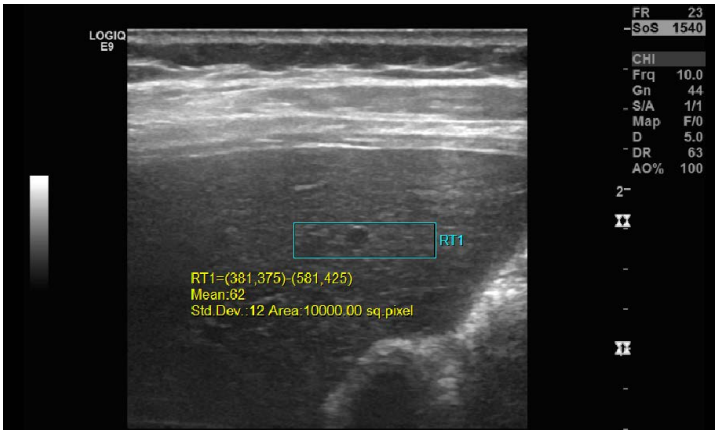

(b)

Figure 3. Two ROIs were selected on a typical ultrasound human liver image with a ML6-15 linear array transducer. One region contains a fully developed speckle, as shown in (a), while the other region contains some specular structures, as shown in (b).

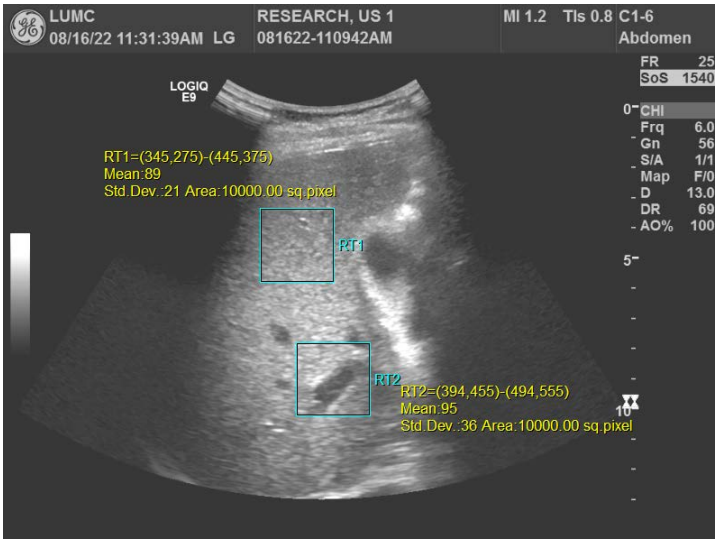

Figure 4. Two ROIs were selected on a typical ultrasound human liver image with a C1-6 curved array transducer. One region contains a fully developed speckle, while the other region contains some specular structures.

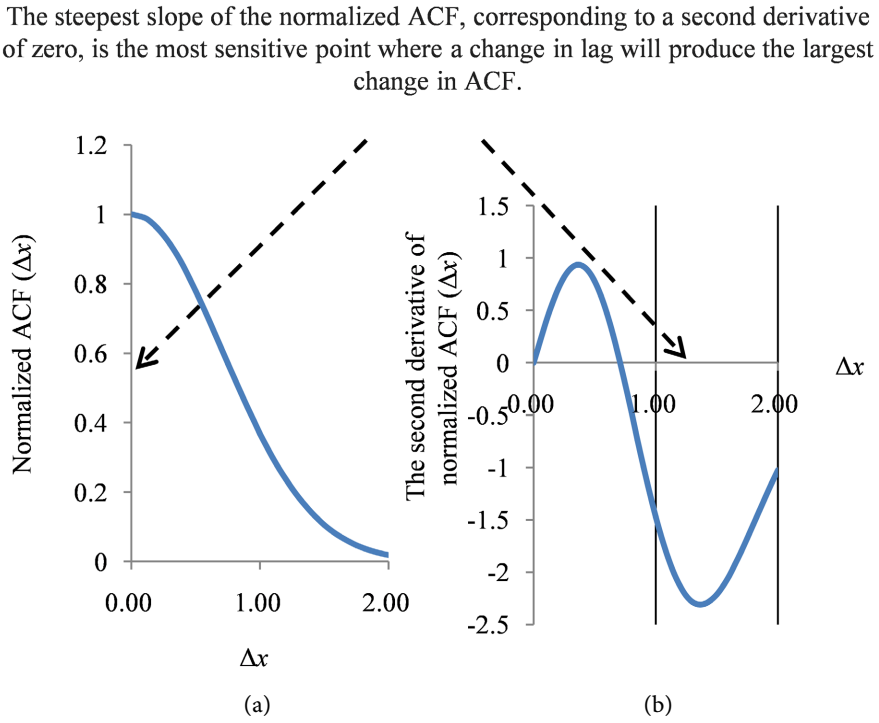

Figure 5. The shape of a typical normalized ACF of ultrasound image data is approximately a Gaussian function as shown in (a). The steepest slope of the normalized ACF, corresponding to a second derivative of zero, is the most sensitive point where a change in lag will produce the largest change in ACF, as shown in (b).

$$1-2a\left(\Delta x\right)^2=0$$

The value of normalized ACF for the most sensitive lag is given by $y=\mathrm{e}^{-1/2}=0.6065$. Here a is the ACF parameter, which not only depends on the spatial resolution of ultrasound image system, but also depends on the ultrasound scattering structure, such as speckle or specular structures. In our study, the most sensitive lag of the normalized ACF were typically in the range of 0.5 mm to 1.0 mm for the images acquired with a ML6-15 transducer, and in the range of 0.5 mm to 2.0 mm for the images acquired with a C1-6 transducer.

3. Results

In our phantom study, the phantom images were acquired using a GE LOGIQ E9 scanner with a ML6-15 linear array transducer. The values of normalized ACF with different lays as well as different SoS settings were computed. When the ROI was in a well-developed speckle region as shown in **Figure 2**, a lag of 0.534 mm was chosen in order to obtain a minimum value of the normalized ACF reaching just below 0.6065 for at least one particular SoS setting. The values of normalized ACF for a lag of 0.534 mm changed with different SoS settings as shown in **Figure 6(a)**. Similarly, when the ROI contained a specular reflector region, also as shown in **Figure 2**, a lag of 0.75 mm was chosen in order to obtain a minimum value of the normalized ACF reaching just below 0.6065 for at least

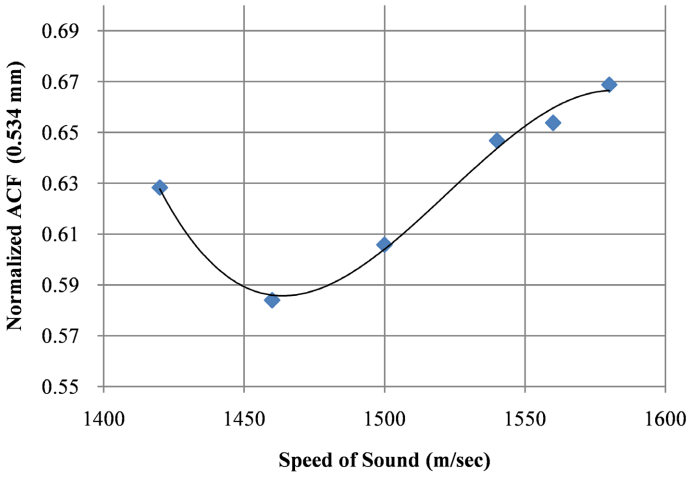

(a)

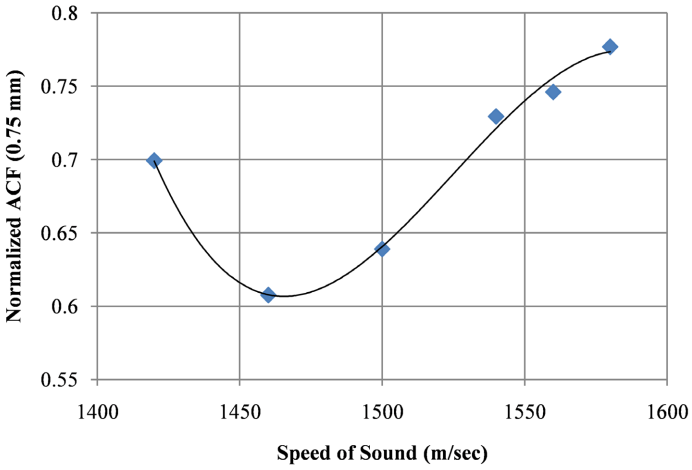

(b)

Figure 6. In our phantom experiment, the normalized ACF with a lag of 0.534 mm as a function of SoS setting for a fully developed speckle is given in (a), while the normalized ACF with a lag of 0.75 mm as a function of SoS setting for a region containing a specular reflector is given in (b).

one particular SoS setting. The results of normalized ACF values with a lag of 0.75 mm in that region varied with different SoS settings are shown in **Figure 6(b)**. Both results show that the minimum value of the normalized ACF is located at SoS = 1460 m/sec, which is very close to the SoS specification of 1450 m/sec provided by the phantom manufacturer. The results demonstrate that both speckle and specular regions can be used to assess SoS in soft tissue. The values of the normalized ACF changed with SoS settings from 1450 m/sec to 1580 m/sec are given in **Table 1**. The results show that the normalized ACF of images containing specular structures, such as the point target here, may be more sensitive to the SoS setting and may provide better SoS estimation results than the ACF of images containing only speckle structures.

In the next step, the ultrasound images of normal human livers were acquired

Table 1. The values of the normalized ACF changed with SoS settings from 1450 m/sec to 1580 m/sec in the ROI containing the fully developed speckle and the specular structures.

SoS settings (m/sec)	1420	1460	1500	1540	1560	1580
Value of Normalized ACF from speckle region	0.6383	0.5839	0.6058	0.6467	0.6537	0.6688
Value of Normalized ACF from specular structure region	0.6992	0.6075	0.639	0.7294	0.746	0.7768

using the same ultrasound scanner with a ML6-15 transducer. The ROIs containing the speckle area as well as some specular structures in the liver image were selected as shown in **Figure 3**. The values of normalized ACF of image data with different lags and different SoS settings were computed. For these images acquired with the ML6-15 transducer, a lag of 0.534 mm was selected in order to get the minimum values of the normalized ACF calculated from a speckle image area reached just below 0.6065, and a lag of 1.10 mm was selected in order to get the minimum values of the normalized ACF calculated from a specular image area reach just below 0.6065. **Figure 7(a)** is the result of the normalized ACF values with a lag of 0.534 mm at different SoS settings, while **Figure 7(b)** is the result of the normalized ACF values with a lag of 1.1 mm at different SoS settings. Both results show that the minimum value of the normalized ACF with the lags of 0.534 mm and 1.10 mm were located at SoS = 1540 m/sec, which is close to the SoS of normal human liver *in vivo*.

Finally, ultrasound images of normal human livers were acquired using the same ultrasound scanner with a C1-6 curved array transducer. As shown in **Figure 4**, the selected ROIs contain speckles as well as some specular structures in the liver images. The values of normalized ACF of image data with different lags and different SoS settings were computed. For these images acquired with a C1-6 curved array transducer, a lag of 1.5 mm was chosen to obtain the minimum value of normalized ACF computed from the speckle image area, which was just below 0.6065, and a lag of 3.0 mm was chosen to get the minimum value of the normalized ACF computed from the specular image area, which was just below 0.6065. **Figure 8(a)** is the result of normalized ACF values with a lag of 1.5 mm at different SoS settings, while **Figure 8(b)** is the result of normalized ACF values with a lag of 1.1 mm at different SoS settings. Both results show that the minimum values of the normalized ACF with lags of 1.5 mm and 3.0 mm are also located at SoS = 1540 m/sec, which is consistent with the results using linear array transducers and close to the SoS of normal human liver *in vivo*.

4. Summary and Discussion

In this paper, a novel image-based method is presented to determine the SoS of soft tissues. The method is based on searching for a minimum of the normalized

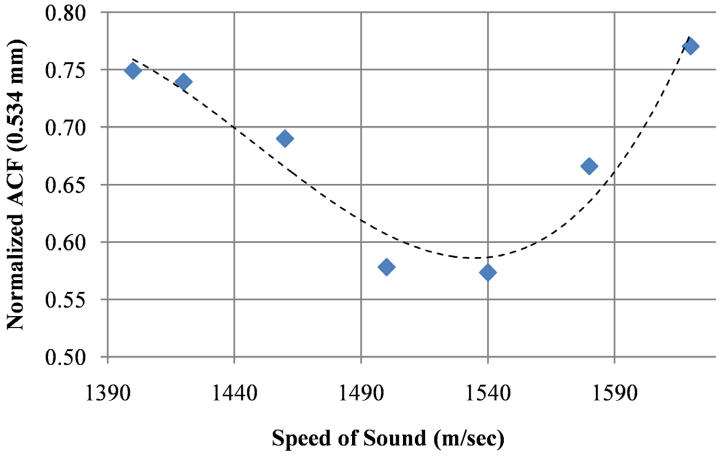

(a)

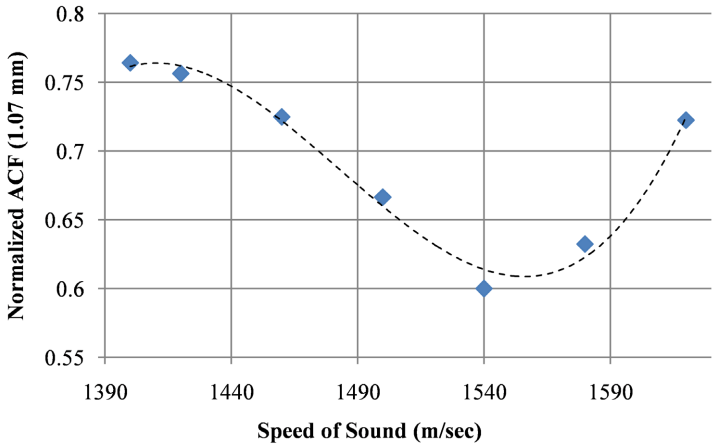

(b)

Figure 7. In our clinical study with a ML6-15 linear array transducer, the normalized ACF with a lag of 0.534 mm as a function of SoS setting for a fully developed speckle is given in (a), while the normalized ACF with a lag of 1.10 mm as a function of SoS setting for a region containing a specular reflector is given in (b).

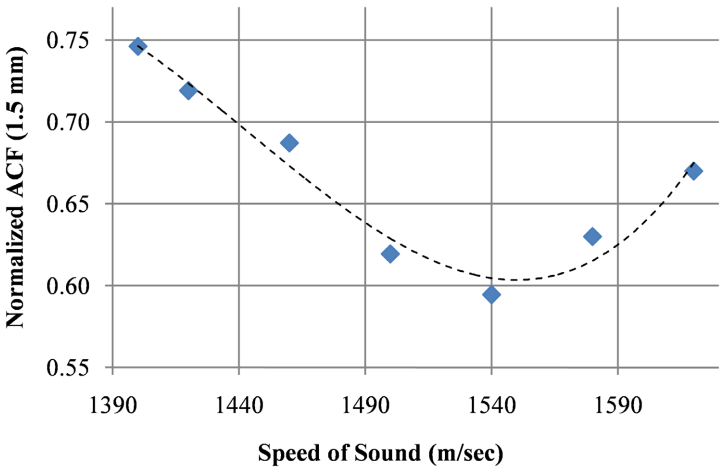

(a)

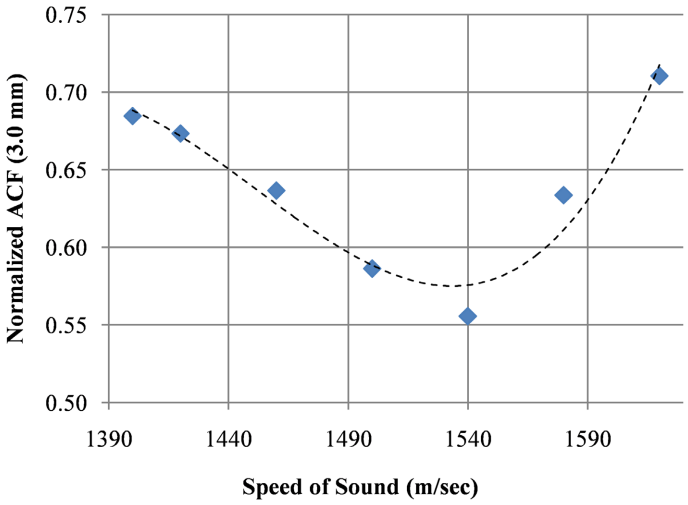

(b)

Figure 8. In our clinical study with a C6-1 curved array transducer, the normalized ACF with a lag of 1.5 mm as a function of SoS setting for a fully developed speckle is given in (a), while the normalized ACF with a lag of 3.0 mm as a function of SoS setting for a region containing a specular reflector is given in (b).

ACF of ultrasound image data with a specific lag among different SoS settings in beamforming channels. The proposed method was validated by imaging a tissue mimicking phantom and normal human liver tissue *in vivo* using a 10 MHz linear array transducer and a 3.5 MHz curved array transducer. If a similar time delay formula can be established for specific transducers, the principle of the method can be generalized to other types of transducers. Our experimental results also show that the lateral resolution of ultrasound images can be noticeably improved if the SoS setting in beamforming channels is close to the real SoS in soft tissues. This means that the minimized ACF value corresponds to maximized image sharpness.

Our method is based on the relative change in normalized ACF of ultrasound image data within a specific ROI and does not require any prior knowledge or assumptions about the ultrasound image, so it is more robust than other methods using RF data processing, which often require adding assumptions such as a reflector or a reference image to find the appropriate time delay.

In real clinical cases, a series of ultrasound images with different SoS settings in beamforming channels should be acquired in a short period of time to avoid changes in the imaging area due to transducer motion and patient motion (e.g. breathing motion). A better approach is to acquire just one set of RF data and then process the same set of RF data in beamforming with different SoS settings to create a series of images. Based on these series of images, our method can then be applied to determine SoS in soft tissues.

Our current study assumes that the effective SoS in soft tissues is uniform, but in reality, the SoS may vary at different locations, such as the body walls with multiple layers of fat and muscle, which may bias the estimation of SoS in the

liver. A method including correction for fat/muscle layer effects has been studied and discussed [9]. The thickness of the fat and muscle layers can be measured by doctors using routine ultrasound. The average SoS used in the calculations could be 1450 m/sec in fat and 1575 m/sec in muscle [10]. Then, in a multi-layer medium, the SoS of different layers is given by

$$\frac{d_{total}}{SoS_{total}} = \frac{d_{muscle}}{SoS_{muscle}} + \frac{d_{fat}}{SoS_{fat}} + \frac{d_{liver}}{SoS_{liver}}$$

where

d_{total} is the depth of ROI, which is used to calculate the normalized ACF,

d_{fat} is the thickness of the fat layer,

SoS_{fat} is the SoS in the fat,

d_{muscle} is the thickness of the muscle layer, and

SoS_{muscle} is the SoS in the muscle.

If $d_{liver} = d_{total} - d_{fat} - d_{muscle}$, and SoS_{liver} is the SoS in the liver, we can determine

$$SoS_{liver} = \frac{d_{liver}}{\frac{d_{total}}{SoS_{total}} - \frac{d_{fat}}{SoS_{fat}} - \frac{d_{liver}}{SoS_{liver}}}$$

In routine clinical examinations, the situation may be more complicated, such as the SoS may not be uniform in soft tissues, strong phase aberration and other image artifacts can degrade the image quality and consequently bias measurement results. The movement of body tissues, which may vary the ROI used to compute the normalized ACF, can produce additional measurement errors.

5. Conclusion

In this paper, a novel image-based method to determine SoS of soft tissue is proposed and validated on both a tissue mimicking phantom and human liver tissue *in vivo* using both linear and curved array transducers. The method is based on searching for a minimum of the normalized ACF of ultrasound image data with a specific lag among different SoS settings in beamforming channels.

Conflicts of Interest

The authors declare no conflicts of interest regarding the publication of this paper.

References

[1] Chen, Q. and Zagzebski, J. (2004) Simulation Study of Effects of Speed of Sound and Attenuation on Ultrasound Lateral Resolution. *Ultrasound in Medicine and Biology*, **30**, 1297-1306. https://doi.org/10.1016/j.ultrasmedbio.2004.07.012

[2] Cho, M.H., Kang, L.H., Kim, J.S. and Lee, S.Y. (2009) An Efficient Sound Speed Es-

timation Method to Enhance Image Resolution in Ultrasound Imaging. *Ultrasonics*, **49**, 774-778. https://doi.org/10.1016/j.ultras.2009.06.005

[3] de Moura, H.L., de Oliveira Silva, V., Guarneri, G.A., Guerreiro, M.T.L., Passarin, T.A.R., Pires, G.P. and Pipa, D.R. (2020) Image-Based Ultrasound Speed Estimation in Isotropic Materials. *IEEE Sensors Journal*, **20**, 12903-12913. https://doi.org/10.1109/JSEN.2020.3002853

[4] Napolitano, D., *et al*. (2006) Sound Speed Correction in Ultrasound Imaging. *Ultrasonics*, **44**, e43-e46. https://doi.org/10.1016/j.ultras.2006.06.061

[5] Chen, J., Yao, L. and Von Behren, P. (1997) Ultrasound System for Estimating the Speed of Sound in Body Tissue. US Patent, Patent Number: 5638820.

[6] Ali, R., Telichko, A.V., Wang, H.J., Sukumar, U.K., Vilches-Moure, J.G., Paulmurugan, R. and Dahl, J.J. (2022) Local Sound Speed Estimation for Pulse-Echo Ultrasound in Layered Media. *IEEE Transactions on Ultrasonics, Ferroelectrics, and Frequency Control*, **69**, 500-511. https://doi.org/10.1109/TUFFC.2021.3124479

[7] Jakovljevic, M., Hsieh, S., Ali, R., Kung, G.C.L., Hyun, D. and Dahl, J.J. (2018) Local Speed of Sound Estimation in Tissue Using Pulse-Echo Ultrasound: Model-Based Approach. *Journal of the Acoustical Society of America*, **144**, 254-266. https://doi.org/10.1121/1.5043402

[8] Treeby, B.E., Varslot, T.K., Zhang, E.Z., Laufer, J.G. and Beard, P.C. (2011) Automatic Sound Speed Selection in Photoacoustic Image Reconstruction Using an Autofocus Approach. *Journal of Biomedical Optics*, **16**, 090501. https://doi.org/10.1117/1.3619139

[9] Imbault, M., Faccinetto, A., Osmanski, B., Tissier, A., Deffieux, T., Gennisson, J., Vilgrain, V. and Tanter, M. (2017) Robust Sound Speed Estimation for Ultrasound-Based Hepatic Steatosis Assessment. *Physics in Medicine & Biology*, **62**, 3582-3598. https://doi.org/10.1088/1361-6560/aa6226

[10] Azhari, H. (2010) Appendix A: Typical Acoustic Properties of Tissues Basics of Biomedical Ultrasound for Engineers. Wiley, New York, 313-314. https://doi.org/10.1002/9780470561478.app1